Oblique incidence properties of locally resonant sonic materials with resonance and Bragg scattering effects

Yuan Bo(袁 博), Wen Ji-Hong(温激鸿), and Wen Xi-Sen(温熙森)†

Vibration and Acoustics Research Group, Laboratory of Science and Technology on Integrated Logistics Support, National University of Defense Technology, Changsha 410073, *China*
MOE Key Laboratory of Photonic and Phononic Crystals, National University of Defense Technology, Changsha 410073, *China*

(Received 21 September 2012; revised manuscript received 30 October 2012)

A locally resonant sonic material (LRSM) is an elastic matrix containing a periodic arrangement of identical local resonators (LRs), which can reflect strongly near their natural frequencies, where the wavelength in the matrix is still much larger than the structural periodicity. Due to the periodic arrangement, an LRSM can also display a Bragg scattering effect, which is a characteristic of phononic crystals. A specific LRSM which possesses both local resonance and Bragg scattering effects is presented. Via the layered-multiple-scattering theory, the complex band structure and the transmittance of such LRSM are discussed in detail. Through the analysis of the refraction behavior at the boundary of the composite, we find that the transmittance performance of an LRSM for oblique incidence depends on the refraction of its boundary and the transmission behaviors of different wave modes inside the composite. As a result, it is better to use some low-speed materials (compared with the speed of waves in surrounding medium) as the LRSM matrix for designing sound blocking materials in underwater applications, since their acoustic properties are more robust to the incident angle. Finally, a gap-coupled LRSM with a broad sub-wavelength transmission gap is studied, whose acoustic performance is insensitive to the angle of incidence.

Keywords: underwater acoustic materials, oblique incidence, locally resonant sonic materials, Bragg scattering

PACS: 43.35.+d, 43.30.+m, 43.20.+g, 43.40.+s **DOI:** 10.1088/1674-1056/22/7/074302

1. Introduction

A locally resonant sonic material (LRSM) is a periodic structural composite which has prominent reflecting or absorbing (if loss is included) behavior in a sub-wavelength frequency region, where the periodic spacing of the structure is still much less than the wavelength in the matrix material. A typical three-dimensional (3D) LRSM consists of an elastic matrix containing periodically arranged local resonators (LRs).[1] The LRs are usually dense metallic spheres coated with soft rubber, whose resonant behavior controls the sub-wavelength performance of the LRSM. In the last decade, LRSM has been widely studied owing to its sub-wavelength blocking behavior.[2–10] However, most of these works focused on the behavior of the local resonance[11–17] and ignored the Bragg scattering effects provided by the periodic structure, as these typically occur at frequencies much higher than those of the resonances. Hence, the periodic arrangement of LRs has not been fully utilized.

Moreover, serving as underwater acoustic materials, LRSMs will encounter oblique incident waves from water surrounding more frequently than normal incidence. However, few researches discussed the acoustic properties of LRSMs under the condition of oblique incidence, except several works analyzed the absolute band gaps of LRSMs.[18–20] As we all know, the oblique acoustic properties of an LRSM is not only determined by the directional band gaps of its infinite counterpart, but also related to the reflection and refraction at the boundary of composite. Therefore, it is quite important to analyze the acoustic performance of LRSMs under the condition of oblique incidences.

In this paper, both local resonance and Bragg scattering effects in a 3D LRSM are analyzed theoretically. The oblique incidence properties of such an LRSM are discussed in detail for the purpose of optimizing the acoustic behavior of LRSMs to be more robust to the incident angle. As a result, an LRSM with low-speed matrix is provided, whose gaps are insensitive to the incident angle. By coupling two kinds of gaps together, such LRSM can possess a broad transmission gap in the sub-wavelength region.

2. Configuration and modelling

For a 3D LRSM, the LRs can be arranged periodically in several different lattices. Here we only consider a rectangular cell arrangement of LRs. Figure 1 shows a section through such a 3D LRSM in a plane normal to the x-direction and passing through the centers of the LRs. In this schematic diagram, the black circles represent the steel cores; the thin annulus around the cores represent the soft coats; the grey background represents the matrix; the dashed lines represent the boundaries of different layers of LRs. The LRs repeat in-

†Corresponding author. E-mail: wenxs@vip.sina.com

© 2013 Chinese Physical Society and IOP Publishing Ltd

finitely in the x and y directions, while the number of layers in the z direction is set to be 8 for transmittance calculations, but to be infinite for complex band structure calculations. The finite LRSM was considered to be surrounded by water. As shown in Fig. 1, the dimension of a cell in x and y directions is called the lattice constant (A) while the dimension in the z direction is referred to as the layer thickness (L); the angle of incidence is θ, which is the angle the incident wave vector makes to the normal of the LRSM interface. It needs to be noted that the incident angle lies in the yz plane for all the calculations in this paper, as it was found that the transmission characteristics for oblique incidence in other planes were very similar.

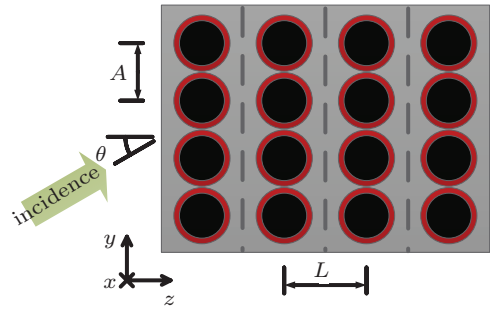


Fig. 1. (color online) A sectional view of the 3D LRSM. The periodicity in x and y directions is called the lattice constant (A); the periodicity in the z direction is named the layer thickness (L); the angle of incidence is referred to as θ.

An LRSM with an epoxy matrix is considered. The density of the epoxy is $\rho = 1180$ kg·m^{-3}, while its longitudinal and shear wave speeds are $c_{\rm L} = 2539$ m·s^{-1} and $c_{\rm S} = 1161$ m·s^{-1}. The lattice constant (A) and layer thickness (L) of the array are set to be 10 mm and 22 mm, respectively. Such arrangement can optimize the band gaps of the composite with border frequency range, and tune the Bragg scattering band gap to the sub-wavelength region, which offers a chance to couple band gaps together in the following discussion. The LRs are lead spheres, 8 mm in diameter, coated in silicone rubber with a thickness of 1 mm. The acoustic properties of the lead are $\rho = 11600$ kg·m^{-3}, $c_{\rm L} = 2493$ m·s^{-1}, and $c_{\rm S} = 1133$ m·s^{-1}, while those of the silicone rubber are $\rho = 1039$ kg·m^{-3}, $c_{\rm L} = 316$ m·s^{-1}, and $c_{\rm S} = 147$ m·s^{-1}. All the materials used are considered lossless, and the transmittance is calculated for the LRSM when it is immersed in water ($\rho = 1000$ kg·m^{-3}, $c_{\rm L} = 1480$ m·s^{-1}). The layer-multiple-scattering theory[21] is used to calculate the complex band structure and the transmittance of the LRSM. During the calculations, an angular-momentum cutoff ($l_{\max} = 4$) for the spherical Bessel function and 33 two-dimensional reciprocal lattice vectors were used. This ensures an error less than 1% in the results.

3. The band structure and the transmittance of the LRSM for normal incidence

Figure 2 shows the complex band structure and the transmittance of the LRSM when the incident wave is normal to the interface. The complex band structure (see Fig. 2(a)) is the relation between the complex wave-number and frequency. The x axis represents the non-dimensional frequency $\Omega = 2fL/c_{\rm ML}$, where $c_{\rm ML}$ is the speed of longitudinal waves in the matrix (2539 m·s^{-1}), and L is the layer thickness (22 mm). When $\Omega = 1$, one half wavelength of longitudinal waves in the matrix is equal to the layer thickness, which occurs at a frequency of 57.7 kHz for the current case.

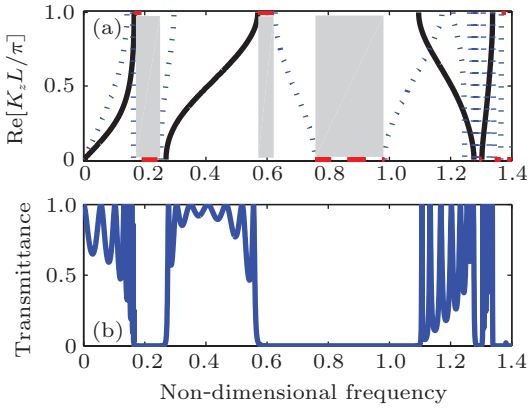


Fig. 2. (color online) (a) The complex band structure and (b) transmittance of the LRSM for normal incidence. The black solid curves represent the dispersion curve for longitudinal waves; the blue dotted curves represent the dispersion curve for shear waves; the shaded areas represent the band gaps.

Here Re$[K_zL/\pi]$ represents the real part of the z component of the complex wave vector which has been reduced by the periodic spacing of the structure. Thanks to the symmetry of the LRSM in the z direction, we only show the positive parts of the reduced wave number, since they are symmetric with their negative parts. The black solid curves in the band structure represent the dispersion curve of longitudinal waves in the composite; the blue dotted curves represent the dispersion curve of shear waves in the composite; the shaded areas indicate the frequency regions where only evanescent waves can propagate in the z direction, since all the wave vectors in these regions are complex. Such regions are known as the band gaps. The red dashed lines inside these band gaps indicate the trajectory of Re$[K_zL]$.

From Fig. 2(a), it can be seen that there are several band gaps existing in the displayed frequency region. According to the analysis of different types of band gaps in Ao's paper,[22] the first band gap in the frequency region of [0.17, 0.25] is recognized as a resonance band gap, since the real part of the complex wave vector (Re$[K_zL]$) jumps from π to 0 inside the gap. In contrast, the band gaps in the frequency regions of [0.57, 0.63] and [0.76, 0.98] are produced by Bragg scattering

effects for both wave modes. This implies that the reflected waves from different layers interfere constructively in these regions for both longitudinal and shear waves. It can be verified by the fact that $\mathrm{Re}[K_z L]$ is always π or 0 inside these band gaps. The phase of $\mathrm{Re}[K_z L]$ is different in the second and third band gaps because they correspond to different orders of Bragg scattering for shear waves. If the dispersion curves of the different modes are considered separately, it is found that the frequency region [0.57, 1.10] is the second forbidden band for longitudinal waves, while the regions [0.30, 0.63] and [0.76, 0.98] are the second and third forbidden bands for shear waves.

Figure 2(b) shows the transmittance of the LRSM with a finite periodicity (8 periods) in the z direction when the incident waves are normal to the composite surface. The solid curve in the figure indicates the ratio of the transmitted intensity to the incident intensity. From Fig. 2(b), it can be seen that the composite has two prominent transmission gaps which are located in [0.17, 0.25] and [0.57, 1.10]. Comparison with the band structure reveals that the first gap is caused by the local resonance as its frequency region coincides with the resonance band gap; the second gap is produced by the Bragg scattering effect for longitudinal waves as its frequency region coincides with the second forbidden band for longitudinal waves in the composite. This implies that the shear modes are not stimulated when longitudinal waves are normally incident on the composite surface. It also can be observed that the transmittance curve always oscillates with frequency whenever it is nonzero. This characteristic is provided by the multiple scattering between two boundaries of the composite, which is well known as Fabry–Pérot-like oscillation. More specifically, the number of peaks for the oscillation in the pass band will be $n-1$, where n is the number of layers of the composite in the z direction ($n = 8$ for this paper).[23] In addition, the layer number (n) will also affect the transmission behavior of the composite. In general, with increasing n, the transmission loss will be more prominent in the regions of band gaps, and the boundaries between pass bands and band gaps will be clearer to distinguish, which is also the reason for this paper to choose the number of layers as 8.

4. Transmission performance of the LRSM for oblique incidence

Figure 3(a) shows the transmittance of the LRSM for oblique incidence as a function of non-dimensional frequency (x axis) and angle of incidence (y axis). The grey scale indicates the transmittance with white indicating total transmission and black total reflection. Figures 3(b)–3(e) demonstrate the transmittance performance of the composite at several specific incident angles, such as 0°, 10°, 45°, and 80°. It can be observed that the transmittance of such an LRSM is strongly dependent on the angle of incidence. As shown in Fig. 3(a), the first transmission gap mentioned in the normal incident case (located in the frequency region [0.17, 0.25]) is not sensitive to the angle of incidence, while the second transmission gap (located initially at [0.57, 1.10]) is. This is because the former gap depends on the local resonance of the LRSM, whose natural frequency depends on the properties of the local resonators. Thus, the angle of incidence will not affect the resonance gap strongly. In contrast, the latter gap is generated purely by Bragg scattering effects in the composite, which requires the periodic spacing of the composite to be an integer multiple of half wavelengths of waves in the structure. Hence, such type of transmission gap is highly dependent on the direction of the waves in the composite, and therefore the incidence angle.

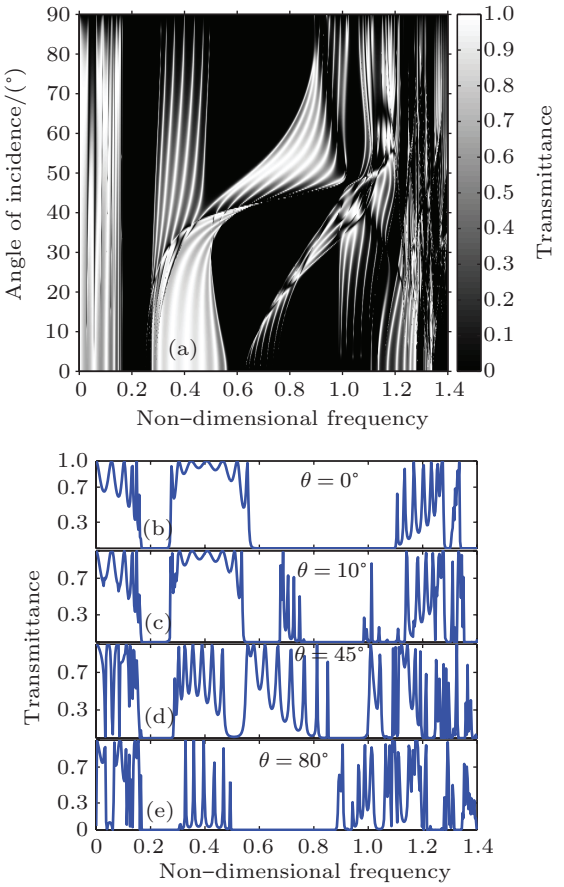


Fig. 3. (color online) (a) The transmittance of the LRSM as a function of the normalized frequency and the angle of incidence. (b)–(e) The transmittance of the composite for specific incident angles.

Moreover, the significance of shear waves increases rapidly with the angle of incidence as shown in Fig. 3(a). This can be verified by the emergence of the pass bands in the frequency regions [0.63, 0.76] and [0.98, 1.17], which can be observed from Fig. 3(c), when the incident angle increases from zero to small angles (less than 10°). These pass bands continue to exist but change in frequency as the angle of incidence increases further. The parallel fluctuations in the transmittance

visible in Fig. 3(a) are the extension of the Fabry–Pérot-like oscillations for different angles of incidence.

In order to understand why the second transmission gap will be so sensitive to the angle of incidence, we analyze the reflection and refraction of waves at the left boundary of the composite. As shown in Fig. 1, the left side of this interface (where the incident waves come from) is a water half space, while the right side of the interface (where the refracted waves propagate into) is the epoxy matrix. Ignoring the scattering behavior of the local resonators in the LRSM, we assume that the right side of the interface is also a half space with properties of the matrix medium. Using Snell's law, we can obtain the angle of refraction by

$$\frac{\sin\theta}{c_0} = \frac{\sin\theta_1}{c_{\mathrm{ML}}} = \frac{\sin\gamma_1}{c_{\mathrm{MS}}}, \tag{1}$$

where θ is the angle of incidence, θ_1 and γ_1 are the angles of refraction for longitudinal and shear waves, c_0 is the speed of sound in water, and c_{ML} and c_{MS} are the speeds of longitudinal and shear waves in the matrix. Using the boundary conditions at the interface, we obtain the reflection and refraction coefficients as[24]

$$\begin{aligned} V &= \frac{Z_{\mathrm{L}}\cos^2 2\gamma_1 + Z_{\mathrm{S}}\sin^2 2\gamma_1 - Z_0}{Z_{\mathrm{L}}\cos^2 2\gamma_1 + Z_{\mathrm{S}}\sin^2 2\gamma_1 + Z_0}, \\ W_{\mathrm{L}} &= \frac{(2\rho_0/\rho_1)\,Z_{\mathrm{L}}\cos 2\gamma_1}{Z_{\mathrm{L}}\cos^2 2\gamma_1 + Z_{\mathrm{S}}\sin^2 2\gamma_1 + Z_0}, \\ W_{\mathrm{S}} &= \frac{-(2\rho_0/\rho_1)\,Z_{\mathrm{S}}\sin 2\gamma_1}{Z_{\mathrm{L}}\cos^2 2\gamma_1 + Z_{\mathrm{S}}\sin^2 2\gamma_1 + Z_0}. \end{aligned} \tag{2}$$

Here, ρ_0 and ρ_1 are the density of water and matrix, $Z_0 = \rho_0 c_0/\cos\theta$ is the characteristic impedance of water, and $Z_{\mathrm{L}} = \rho_1 c_{\mathrm{ML}}/\cos\theta_1$ and $Z_{\mathrm{S}} = \rho_1 c_{\mathrm{MS}}/\cos\gamma_1$ are the characteristic impedances of the matrix for longitudinal and shear waves. In addition, V represents the reflection coefficient, while W_{L} and W_{S} represent the refraction coefficients for longitudinal and shear waves, respectively. These coefficients contain both amplitude and phase information. In order to acquire the intensity coefficients, we need to substitute them into the following formulas:

$$R = |V|^2, \quad T_{\mathrm{L}} = \frac{\rho_1\tan\theta}{\rho_0\tan\theta_1}|W_{\mathrm{L}}|^2, \quad T_{\mathrm{S}} = \frac{\rho_1\tan\theta}{\rho_0\tan\gamma_1}|W_{\mathrm{S}}|^2. \tag{3}$$

Here, R is the intensity ratio of the reflected wave relative to the incident wave, while T_{L} and T_{S} are the intensity ratios for the refracted longitudinal and shear waves, respectively. The sum of these three coefficients will always equal one ($R + T_{\mathrm{L}} + T_{\mathrm{S}} = 1$) in order to obey the law of energy conservation.

Figure 4 shows the angles of refraction and the energy flux coefficients for the reflected and refracted waves at the left boundary of the LRSM as a function of the angle of incidence. It can be observed from Fig. 4(a) that the longitudinal refracted wave has a critical angle of incidence of 35.7°. If $\theta > 35.7°$, no longitudinal waves can refract into the matrix from the left surface of the LRSM. Such a phenomenon is known as total internal reflection. In contrast, the shear refracted wave does not have such critical angle since the shear speed of the matrix (1161 m·s^{-1}) is slower than the speed of sound in water.

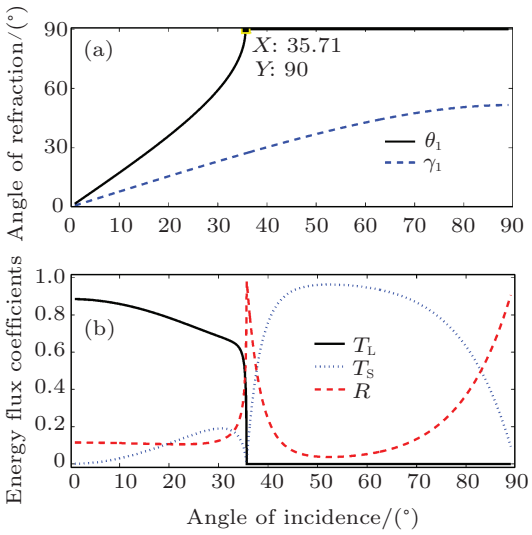


Fig. 4. (color online) (a) The refraction angles and (b) intensity ratios for reflection and refraction at the boundary of the LRSM matrix.

Figure 4(b) demonstrates what happens to the energy flux coefficients around the critical angle. As shown in this subfigure, most of the energy initially belongs to the longitudinal refracted wave when $\theta = 0°$, while the rest of the energy is reflected by the interface. With increasing angle of incidence, a part of the refracted energy is transferred to the shear mode from the longitudinal mode. However, the portion of the energy in the shear wave never exceeds 20% for angles of incidence below the critical angle. When the incident angle is 35.7°, the energy coefficient of the longitudinal refracted waves plummets to zero, and most of the incident energy is reflected at the interface. As the incident angle increases further, most of the incident energy is transferred to the refracted shear wave, and no longitudinal waves will propagate into the matrix.

In order to investigate the angular effect further, Fig. 5 shows the transmittance of such an LRSM for the case when the composite is surrounded by a material with the properties of the matrix (epoxy). This enables the incident waves to be either longitudinal waves (Fig. 5(a)) or shear waves (Fig. 5(b)). Both subfigures have the same non-dimensional frequency as their x axes, the angle of incidence as their y axes, and the same grey scale to indicate their transmittance. Although both Figs. 3(a) and 5(a) are for oblique longitudinal waves, their surrounding media are different. The latter case does not have an interface at the boundary of the LRSM, so total internal reflection does not occur. Comparing Fig. 3(a) with Fig. 5(a),

one can see that the two transmission gaps in the frequency regions [0.17, 0.25] and [0.57, 1.10] exist for both cases when $\theta = 0°$. However, the second transmission gap (Bragg type) is more insensitive to the incident angle when the surrounding medium is epoxy. In contrast, the transmission performance of the Bragg gap for shear incident case (see Fig. 5(b)) located in the region of [0.57, 1.10] is similar to the counterpart in Fig. 3(a). This gap temporarily vanishes when the incident shear wave angle is around 30°–40°. Moreover, when $\theta = 0°$, the frequency regions of the transmission peaks and gaps in Fig. 5(b) coincide with the pass and forbidden bands of shear waves in the band structure (see Fig. 2(a)).

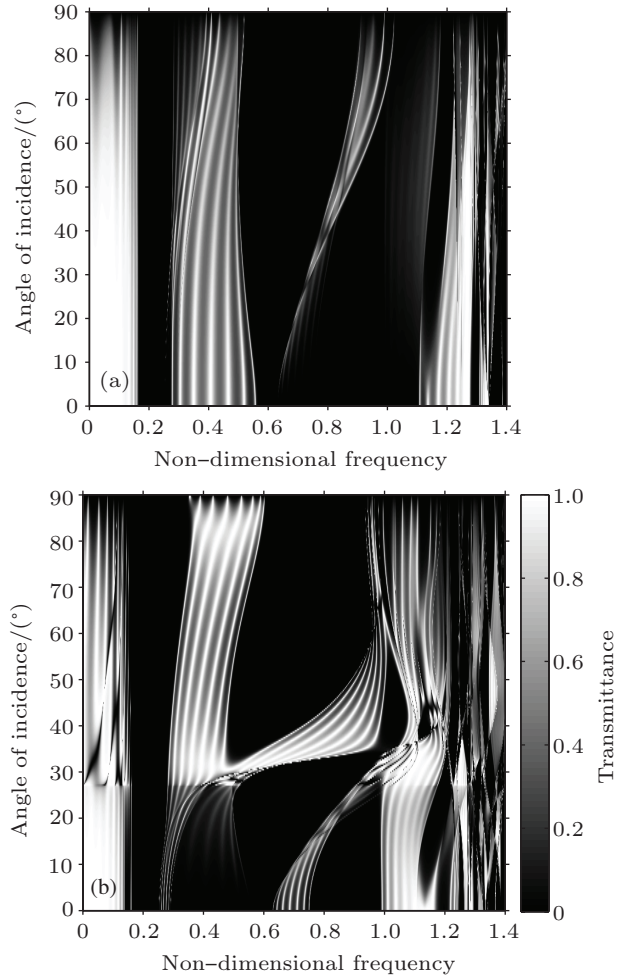


Fig. 5. The transmittance properties of the 8-period LRSM when surrounded by an elastic medium with the same elastic properties as the matrix material. Results are shown for incident (a) longitudinal and (b) shear waves.

In general, the transmittance performance of the LRSM in Fig. 3(a) is the result of the combined effects of refraction at the interface and the transmission behavior for different wave-modes. When the LRSM is surrounded by water and the incidence angle is less than the critical angle, the waves refracted at the interface are mainly longitudinal. Hence, the transmittance of the LRSM mainly depends on the transmission behavior of longitudinal waves in the composite (see Fig. 5(a)). Since the obliquity of incoming waves are enlarged at the boundary of composite, Fig. 5(a) will only provide the transmittance performance of the LRSM for $\theta \in [0°, 35.7°]$. Otherwise, if the incident angle is larger than the critical angle, the shear mode will dominate. Therefore, the transmittance of the LRSM immersed in water will mainly depend on the transmission behavior of shear waves inside the composite (see Fig. 5(b)). More specifically, when $\theta \in [35.7°, 90°]$, the angle of shear waves in the composite can only range from 27° to 52° according to the refraction angle shown in Fig. 4(a).

In addition, it can be seen that the high reflection of the interface around the critical incident angle (see Fig. 4(b)) does not affect the transmittance of the LRSM significantly. The waves near the incident angle of 35.7° can still propagate through the LRSM efficiently for certain frequencies. This is because the periodicity of the composite and the multiple scattering between its two boundaries reinforce the reflections from different layers of scatterers, thus eventually cancel out the highly reflecting behavior at the left boundary of the composite.

Although only one specific case has been discussed here, a number of different types of LRSMs have been investigated as part of the research programme. It has been observed that the transmittance performance of an LRSM always depends on the refraction at its interface and the transmission behavior of different wave modes. Furthermore, the overall transmission behaviors of shear waves are usually more sensitive to the incident angle than that of longitudinal waves. Therefore, if an LRSM is designed for the purpose of blocking sound in water from any direction, its matrix should use a low-speed material to avoid the stimulation of shear waves. The so-called low-speed material is relative to the sound speed of the surrounding materials. If the speeds of both wave modes in the matrix are slower than the sound speed of the surrounding medium, neither wave mode will encounter the total internal reflection in the oblique incident case, and more energy will be transferred into the refracted longitudinal wave mode rather than refracted shear mode or reflected waves.

Figure 1 can also be considered to show an instance of such an LRSM with a low-speed matrix. In this case, all of the acoustic properties and structural parameters keep the same as previously, except that the matrix is replaced with a type of natural rubber with $\rho = 1300\ \mathrm{kg{\cdot}m^{-3}}$, $c_\mathrm{L} = 1140\ \mathrm{m{\cdot}s^{-1}}$, and $c_\mathrm{S} = 219\ \mathrm{m{\cdot}s^{-1}}$. Figure 6(a) shows the angles of refraction as functions of the angle of incidence at the left boundary of the natural rubber matrix. Figure 6(b) shows the intensity ratios of reflected and refracted waves at this interface. Figure 6(c) shows the transmittance of this LRSM for oblique incidence.

From Fig. 6(b), it can be seen that the energy coefficient of the refracted shear wave (T_S) is almost zero regardless of the incident angle, which means no energy is transferred into

the shear mode at the boundary of the composite. Moreover, figure 6(a) shows that both refracted angles of longitudinal and shear waves are smaller than their corresponding incident angles. This implies that the obliquities of the incoming waves are reduced after passing through the boundary of matrix. Both of these factors facilitate the transmittance performance of the LRSM to be more robust to the angle of incidence. Figure 6(c) shows the transmittance image of this LRSM with a rubber matrix for oblique incidence. The transmission gap in the frequency region of [0.35, 0.56] is produced by local resonance, while the gap in the region of [0.58, 0.93] is induced by the Bragg scattering effect. The parallel fluctuation between two transmission gaps (in the region of [0.56, 0.58]) demonstrates the efficient propagation of waves for different incident angles. It can be seen that the second transmission gap is much more insensitive to the oblique incidence than the previous case (see Fig. 3(a)).

Figure 7 shows the transmission behaviors of longitudinal and shear waves inside such an LRSM. By comparing Fig. 6(c) and Fig. 7(a), we can find that the transmittance performance of such LRSM in water surrounding is similar to its transmission behavior of longitudinal wave inside the composite. This verified the conclusion that only longitudinal waves are stimulated at the boundary of composite. On the contrary, the transmission behavior of shear wave exhibits strong sensitivity to the angle of incidence, which is shown in Fig. 7(b). However, it has never been excited when the incident wave is oblique longitudinal wave from water surrounding.

In addition, as shown in Fig. 6(c), the Bragg gap (in the region of [0.58, 0.93]) is already close to the resonance gap (in the region of [0.35, 0.56]). By tuning the resonant frequency of LRs to couple two kinds of gaps together, we can obtain an optimized LRSM with broad sub-wavelength transmission gap. Figure 7(c) shows the transmittance performance of the gap-coupled case. The shear speed of coat has been varied to 178 $\mathrm{m{\cdot}s^{-1}}$, while all the other parameters remain the same as previous LRSM with low-speed matrix. Such gap-coupled case exhibits an integrated transmission gap in the region of [0.34, 0.93], which is also robust to the angle of incidence.

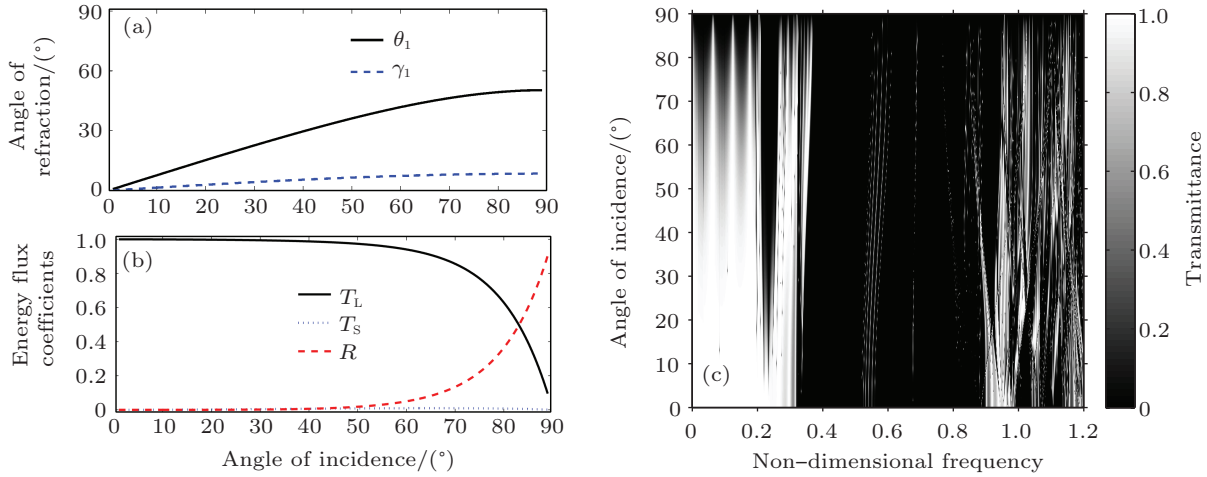


Fig. 6. (color online) (a) The angles of refraction and (b) the intensity ratios of reflected and refracted waves at the left surface of the natural rubber matrix. (c) Transmittance of an LRSM based on this natural rubber matrix for oblique incidence.

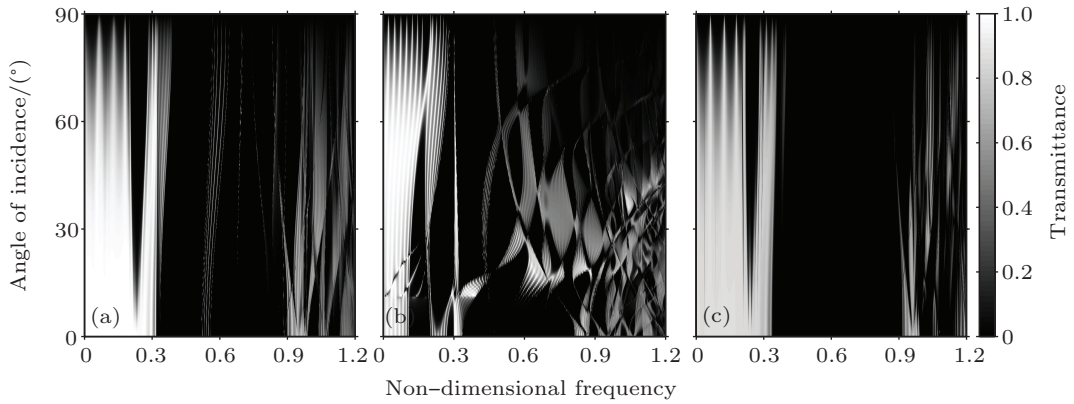


Fig. 7. The transmission behaviors of the (a) longitudinal and (b) shear waves for the LRSM with a low-speed matrix, and (c) the transmittance of gap-coupled LRSM.

5. Conclusion

This paper has discussed the acoustic properties of 3D LRSMs for use in water and their performance for oblique incidence. The complex band structure and the transmittance of a specific LRSM has been analyzed in detail using the layer-multiple-scattering theory. Through investigation of the refraction behavior at the boundary of the composite, we have observed that the transmittance performance of an LRSM depends on the refraction at its surface and the transmission behavior of different wave modes inside the composite. For most high-speed materials (compared with the speeds of waves in surrounding medium), there will be a critical angle for the incoming waves, and the acoustic properties of these LRSMs are usually sensitive to the incident angle. In contrast, LRSMs with low-speed matrices are more suitable for designing sound blocking materials, since their acoustic properties are more robust to the angle of incidence. As a result, a gap-coupled LRSM with low-speed matrix is analyzed. Such composite exhibits a broad sub-wavelength transmission gap regardless of incident angle, which has a good application prospect for the underwater acoustic materials.

Acknowledgments

Yuan Bo acknowledges the support of the China Scholarship Council for funding him to study at the University of Southampton in the UK, and also appreciates his supervisor Victor F. Humphrey for his earnest guidance and help.

References

[1] Liu Z, Zhang X, Mao Y, Zhu Y, Yang Z, Chan C and Sheng P 2000 *Science* **289** 1734
[2] Goffaux C, Sánchez-Dehesa J and Lambin P 2004 *Phys. Rev. B* **70** 184302
[3] Wang G, Wen X, Wen J, Shao L and Liu Y 2004 *Phys. Rev. Lett.* **93** 154302
[4] Hirsekorn M 2004 *Appl. Phys. Lett.* **84** 3364
[5] Liu Z, Chan C T and Sheng P 2005 *Phys. Rev. B* **71** 014103
[6] Hirsekorn M, Delsanto P, Leung A and Matic P 2006 *J. Appl. Phys.* **99** 124912
[7] Yu D L, Wang G, Liu Y Z, Wen J H and Qiu J 2006 *Chin. Phys.* **15** 266
[8] Liu Z, Yang S and Zhao X 2005 *Chin. Phys. Lett.* **22** 3107
[9] Zhao H, Wen J, Liu Y, Yu D, Wang G and Wen X 2008 *Chin. Phys. B* **17** 1305
[10] Wen J, Yu D, Liu J, Xiao Y and Wen X 2009 *Chin. Phys. B* **18** 2404
[11] Qin B, Chen J and Cheng J 2005 *Chin. Phys.* **14** 2522
[12] Wang G, Liu Y Z, Wen J H and Yu D L 2006 *Chin. Phys.* **15** 407
[13] Wang G, Shao L H, Liu Y Z and Wen J H 2006 *Chin. Phys.* **15** 1843
[14] Zhao H, Liu Y, Wen J, Yu D, Wang G and Wen X 2006 *Chin. Phys. Lett.* **23** 2132
[15] Zhao H, Liu Y, Wen J, Yu D and Wen X 2007 *Phys. Lett. A* **367** 224
[16] Wen J, Zhao H, Lü L, Yuan B, Wang G and Wen X 2011 *J. Acoust. Soc. Am.* **130** 1201
[17] Jiang H, Wang Y, Zhang M, Hu Y, Lan D, Wu Q and Lu H 2010 *Chin. Phys. B* **19** 026202
[18] Larabi H, Pennec Y, Djafari-Rouhani B and Vasseur J 2007 *Phys. Rev. E* **75** 066601
[19] Kuang W, Hou Z, Liu Y and Li H 2006 *J. Phys. D: Appl. Phys.* **39** 2067
[20] Sainidou R, Djafari-Rouhani B, Pennec Y and Vasseur J 2006 *Phys. Rev. B* **73** 024302
[21] Sainidou R, Stefanou N, Psarobas I and Modinos A 2005 *Comp. Phys. Comm.* **166** 197
[22] Ao X and Chan C T 2009 *Phys. Rev. B* **80** 235118
[23] James R, Woodley S, Dyer C and Humphrey V 1995 *J. Acoust. Soc. Am.* **97** 2041
[24] Brekhovskikh L M 1980 *Waves in Layered Media* (2nd edn.) (New York: Academic Press) pp. 43–46